

A Kernel Theory of Modern Data Augmentation

Tri Dao¹, Albert Gu¹, Alexander J. Ratner¹, Virginia Smith¹, Christopher De Sa², and Christopher Ré¹

¹Department of Computer Science, Stanford University

²Department of Computer Science, Cornell University

{trid,albertgu,ajratner,smithv}@stanford.edu, cdesa@cs.cornell.edu,
chrismre@cs.stanford.edu

January 3, 2022

Abstract

Data augmentation, a technique in which a training set is expanded with class-preserving transformations, is ubiquitous in modern machine learning pipelines. In this paper, we seek to establish a theoretical framework for understanding modern data augmentation techniques. We start by showing that for kernel classifiers, data augmentation can be approximated by first-order feature averaging and second-order variance regularization components. We connect this general approximation framework to prior work in invariant kernels, tangent propagation, and robust optimization. Next, we explicitly tackle the compositional aspect of modern data augmentation techniques, proposing a novel model of data augmentation as a Markov process. Under this model, we show that performing k -nearest neighbors with data augmentation is asymptotically equivalent to a kernel classifier. Finally, we illustrate ways in which our theoretical framework can be leveraged to accelerate machine learning workflows in practice, including reducing the amount of computation needed to train on augmented data, and predicting the utility of a transformation prior to training.

1 Introduction

The process of augmenting a training dataset with synthetic examples has become a critical step in modern machine learning pipelines. Data augmentation aims to artificially create new training data by applying transformations such as rotations or crops to input data while preserving the class labels. This practice has many potential benefits: Data augmentation can encode prior knowledge about data or task-specific invariances; act as regularizer to make the resulting model more robust; and provide resources to data-hungry deep learning models. As a testament to its growing importance, the technique has been used to achieve nearly all state-of-the-art results in image recognition [1, 6, 9, 23], and is becoming a staple in other areas as well [30, 15].

Despite its ubiquity and importance to the machine learning process, data augmentation is typically performed in an ad-hoc manner with little understanding of the underlying theoretical implications. Moreover, manually configuring a new data augmentation pipeline is arduous, as it requires selecting not only which transformations to apply, but also the order in which they are applied, and the hyperparameters of each transformation. In the field of deep learning, a common understanding of data augmentation is that it acts as a regularizer by increasing the number of data points and constraining the model [8, 31]. However, even for simpler models, it is not well-understood how training on augmented data affects the parameters and decision surface of the model, and how different data transformations compose with one another.

We make a step towards answering both of these questions. First, we show that a kernel classifier on augmented data approximately decomposes into two components: (i) a smoothed version of the transformed features, and (ii) a data-dependent variance regularization term. This suggests a more nuanced explanation

of data augmentation—namely, that it improves generalization *both by increasing coverage (i.e., the types of data/features exposed to the model) and by reducing model complexity*. We validate the quality of our proposed approximation empirically, showing the objective value stays within 6% of the true objective throughout training, and with 99.8% overlap in predictions. We also draw connections to other generalization-improving techniques, including recent work in invariant learning [32] and robust optimization [18].

Second, we analyze a novel model of data augmentation as a Markov process that more closely matches the way it is performed in practice—via a random sequence of composed transformations. We show that performing k -nearest neighbors with this model asymptotically results in an kernel classifier, where the kernel is a function of the base augmentations. Our results provide insight into how augmentation affects the learned representation of the original data.

Finally, we demonstrate the practical utility of our theoretical understanding of data augmentation. While our analysis considers kernel classifiers, we also explore the insight gained on deep learning pipelines, showing that our approximation can reduce training computation by 30%, while realizing 92% of the accuracy gain. We also use our theory to develop a diagnostic that determines the importance of a transformation prior to training.

2 Related Work

Data augmentation has long played an important role in machine learning. For many years it has been used, for example, under the guises of *jittering* and *virtual examples* in the neural network and kernel methods literatures [25, 24, 3]. These methods aim to augment or modify the raw training data so that the learned model will be invariant to known transformations or perturbations. There has also been significant work in incorporating invariance directly into the model or training procedure, rather than by expanding the training set. One illustrative example is that of tangent propagation for neural networks [26, 27], which proposes a regularization penalty to enforce local invariance, and has been extended in several recent works [22, 4, 32]. However, while efforts have been made that loosely connect traditional data augmentation with these methods [14, 32], there has not been a rigorous study on how these sets of procedures relate in the context of modern models and transformations.

In this work, we make the connection between augmentation and modifications to the model explicit, and show that prior work on tangent propagation can be derived as a special case of our more general theoretical framework (Section 5). Moreover, we draw connections to recent work in variance regularization [16] and robust optimization [18], illustrating that data augmentation not only affects the model by increasing coverage of invariant forms, but also by reducing the variance of the estimator. These analyses lead to an important insight into how invariance can be most effectively applied in deep learning architectures (Section 5), which we show can be used to reduce training computation and diagnose the effectiveness of various transformations.

Prior theory also does not model the complex process by which data augmentation is often applied—namely, through a sequence of numerous composed transformations. For example, a common recipe in achieving state-of-the-art accuracy in image classification pipelines is to apply a sequence of transformations such as crops, flips, or local affine transformations to the training data, with parameters drawn randomly from hand-tuned ranges [1, 5]. Similar strategies have also been employed in applications of classification for audio [30] and text [15].

Unfortunately, when applying transformations in this manner, traditional assumptions on locality and differentiability of the transformations can quickly become invalid [11, 19]. In this more realistic setting, there has been recent work that aims to develop empirical methodologies and heuristics for learning how to tune and compose long sequences of transformations [28, 7, 21]. However, there remains a dearth of theory to capture this process, particularly in determining how sequences of transformations affect the resulting model.

In Section 4, we analyze a motivating model reaffirming the connection between augmentation and kernel methods, even in the setting of complex composed transformations. While the connection between data augmentation and kernels has been previously observed, it is typically explored in the context of simple

geometrical invariances with closed forms. Furthermore it is often approached in the opposite direction—by looking for kernels that satisfy certain invariance properties [11]. In this work, we instead approach the connection starting directly from data augmentation, and demonstrate that even complicated augmentation procedures akin to those used in practice can be represented as a kernel method.

3 The Effect of Augmentation: Coverage and Regularization

It is commonly understood that data augmentation can be viewed as a regularizer, in that it reduces generalization error but not necessarily training error [8, 31]. We make this more precise, showing that data augmentation has two specific effects: (i) increasing the coverage of augmented forms by averaging the features of augmented data points, and (ii) penalizing model complexity via a variance regularization term. Our theory applies to a general augmentation process (Section 3.1), and we demonstrate connections to prior work throughout our derivation of the feature averaging (Section 3.2) and variance regularization (Section 3.3) components. We validate our theory empirically (Section 3.4), and in Section 5, we show the practical utility of our analysis to both kernel and deep learning pipelines.

3.1 General Augmentation Process

To illustrate the effects of augmentation, we explore it in conjunction with a general kernel classifier. In particular, suppose that we have an original kernel K with a (for simplicity’s sake) finite-dimensional feature map $\phi : \mathbb{R}^n \rightarrow \mathbb{R}^m$, and we aim to minimize some smooth convex loss $l : \mathbb{R} \times \mathbb{R} \rightarrow \mathbb{R}$ with parameter $w \in \mathbb{R}^m$ over a dataset $(x_1, y_1), \dots, (x_N, y_N)$. The original objective function to minimize is $f(w) = \frac{1}{N} \sum_{i=1}^N l(w^\top \phi(x_i); y_i)$. Two common examples are logistic regression $l(\hat{y}; y) = \log(1 + \exp(-y\hat{y}))$ and linear regression $l(\hat{y}; y) = (\hat{y} - y)^2$.

Now, suppose that we augment the dataset using an augmentation kernel T . That is, for each data point x_i , there is a distribution $T(x_i)$ over data points into which x_i can be transformed. The new expected objective function becomes:

$$g(w) = \frac{1}{N} \sum_{i=1}^N \mathbf{E}_{z_i \sim T(x_i)} [l(w^\top \phi(z_i); y_i)]. \quad (1)$$

3.2 Data Augmentation as Feature Averaging

Suppose that the applied augmentations are “local” in the sense that they don’t significantly modify the feature map ϕ . Using the first-order Taylor approximation, we can expand each term around any point ϕ_0 that doesn’t depend on z_i :

$$\mathbf{E}_{z_i \sim T(x_i)} [l(w^\top \phi(z_i); y_i)] \approx l(w^\top \phi_0; y_i) + \mathbf{E}_{z_i \sim T(x_i)} [w^\top (\phi_0 - \phi(z_i))] l'(w^\top \phi_0; y_i).$$

Picking $\phi_0 = \mathbf{E}_{z_i \sim T(x_i)} [\phi(z_i)]$, the second term vanishes:

$$g(w) \approx \hat{g}(w) := \frac{1}{N} \sum_{i=1}^N l(w^\top \mathbf{E}_{z_i \sim T(x_i)} [\phi(z_i)]; y_i). \quad (2)$$

If we define $\psi(x) = \mathbf{E}_{z \sim T(x)} [\phi(z)]$, i.e., the average feature of all the transformed versions of x , then $\hat{g}(w) = \frac{1}{N} \sum_{i=1}^N l(w^\top \psi(x_i); y_i)$. This is exactly the objective of a linear model with a new feature map ψ . We call this the *first-order approximation*. If we overload notation and use $T(x, u)$ to denote the probability

density of transforming x to u , this new feature map corresponds to a new kernel:

$$\begin{aligned}
\bar{K}(x, x') &= \langle \psi(x), \psi(x') \rangle \\
&= \langle \mathbf{E}_{u \sim T(x)} [\phi(u)], \mathbf{E}_{u' \sim T(x')} [\phi(u')] \rangle \\
&= \int_{u \in \mathbb{R}^n} \int_{u' \in \mathbb{R}^n} \langle \phi(u), \phi(u') \rangle T(x, u) T(x', u') du' du \\
&= \int_{u \in \mathbb{R}^n} \int_{u' \in \mathbb{R}^n} K(u, u') T(x, u) T(x', u') du' du \\
&= (TKT^\top)(x, x').
\end{aligned}$$

That is, training a kernel linear classifier with a particular loss function plus data augmentation is equivalent, to first order, to training a linear classifier with the same loss on an augmented kernel $\bar{K} = TKT^\top$. This new kernel has the effect of increasing the coverage of the model, as the model is exposed to features from transformed input that are not necessarily present in the original training set.

By Jensen's inequality, since the function l is convex, $\hat{g}(w) \leq g(w)$. In other words, if we solve the optimization problem that results from data augmentation, the resulting objective value using \bar{K} will be no larger. Further, if we assume that the loss function is strongly convex and strongly smooth, we can quantify how much the solution to the first-order approximation and the solution of the original problem with augmented data will differ (see Proposition 2 in the appendix). We explore the accuracy of this first-order approximation empirically in Section 3.4.

3.3 Data Augmentation as Variance Regularization

Next, we show that the second-order approximation of the objective on an augmented dataset is equivalent to variance regularization, making the classifier more robust. We can get an exact expression for the error by considering the second-order term in the Taylor expansion, with ζ_i denoting the remainder function from Taylor's theorem:

$$\begin{aligned}
g(w) - \hat{g}(w) &= \frac{1}{2N} \sum_{i=1}^N \mathbf{E}_{z_i \sim T(x_i)} \left[\left(w^\top (\phi(z_i) - \psi(x_i)) \right)^2 l''(\zeta_i(w^\top \phi(z_i)); y_i) \right] \\
&= w^\top \left(\frac{1}{2N} \sum_{i=1}^N \mathbf{E}_{z_i \sim T(x_i)} \left[\Delta_{z_i, x_i} \Delta_{z_i, x_i}^\top l''(\zeta_i(w^\top \phi(z_i)); y_i) \right] \right) w,
\end{aligned}$$

where $\Delta_{z_i, x_i} := \phi(z_i) - \psi(x_i)$ is the difference between the features of the transformed image z_i and the averaged features $\psi(x_i)$. If (as is the case for logistic and linear regression), l'' is independent of y , the error term is independent of the labels. That is, our original augmented objective g is the modified objective \hat{g} plus some regularization that is a function of the training examples, but *not the labels*. In other words, data augmentation has the effect of performing *data-dependent regularization*.

The second-order approximation to the objective is given by

$$\tilde{g}(w) := \hat{g}(w) + \frac{1}{2N} \sum_{i=1}^N w^\top \mathbf{E}_{z_i \sim T(x_i)} [\Delta_{z_i, x_i} \Delta_{z_i, x_i}^\top] l''(w^\top \psi(x_i)) w. \quad (3)$$

For a fixed w , this error term is exactly the variance of the estimator, where we assume that the true data X can be sampled from the empirical data points x_i and their augmented versions, specified by $T(x_i)$, weighted by $l''(w^\top \psi(x_i))$.

Connections to prior work. Previous work [16] bounds generalization error in terms of the empirical loss and the variance of the estimator. Therefore the second-order objective here is optimizing generalization and automatically balancing bias (empirical loss) and variance. Though the resulting problem is generally non-convex, it can be approximated by a distributionally robust convex optimization problem [18], which can be

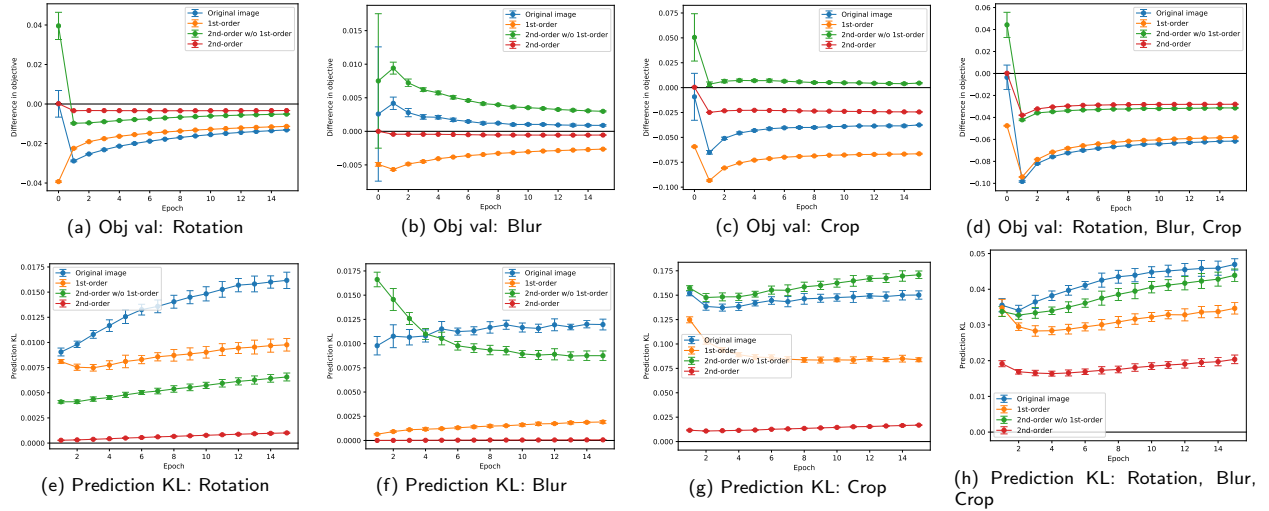


Figure 1: The difference in objective value (a-d) and prediction distribution (e-h) (as measured via the KL divergence) between approximate and true objectives. In all plots, the second-order approximation is much closer to the true objective than the first-order approximation, demonstrating that the variance regularization term (Section 3.3) plays a key role. While the approximations all perform reasonably well on “local” transformations such as rotation and blur (left), they do not model the objective as accurately for non-local transformations, or sequences of composed transformations (right). We explore a more general analysis of these complex augmentations in Section 4.

efficiently solved by a stochastic procedure [17]. Moreover, in Section 5, we show that when applied to neural networks, the described second-order objective can realize classical tangent propagation methods [26, 27, 32] as a special case. More precisely, the second-order only term (green) in Figure 1 is equivalent to the approximation described in [32], where it was described in the context of neural networks. Our results indicate that considering both the first- and second-order terms results in a more accurate approximation of the true objective.

3.4 Validation

We empirically validate¹ the first- and second-order approximations, $\hat{g}(w)$ (2) and $\tilde{g}(w)$ (3), comparing to the actual objective of the model trained with augmented data $g(w)$ (1) on MNIST, using rotation, crop, or blur—using either an RBF kernel (with random Fourier features [20]) or LeNet (see details in Appendix E.1). Our results show that while both approximations perform reasonably, the second-order approximation indeed results in a better approximation of the actual objective, validating the significance of the variance regularization component of data augmentation. Moreover, we note that the “local” transformations of small rotations and Gaussian blur tend to be better captured by our approximation, thus validating the assumptions made in Section 3.2, *but also illustrating the need to better understand more complex transformations* (a task we explore in Section 4).

In Figure 1(a-d), we plot the difference between the actual objective function over augmented data $g(w)$ and: (i) the first-order approximation $\hat{g}(w)$, (ii) second-order approximation $\tilde{g}(w)$, and (iii) second-order approximation without the first-order term, $f(w) + (\tilde{g}(w) - \hat{g}(w))$. As a baseline, we also plot the difference between the augmented objective and over non-augmented data (i.e., original image), $f(w)$. In Figure 1(e-h), we plot the Kullback–Leibler divergence between the distribution over classes predicted by the actual model and the approximate models. In terms of both objective value and prediction distribution, while both first- and second-order approximations do well in approximating the actual model, the second-order

¹Code to reproduce experiments and plots is available at https://github.com/HazyResearch/augmentation_code

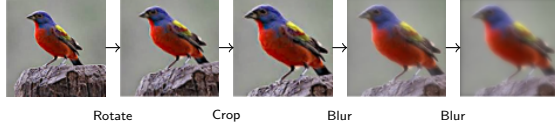


Figure 2: An example of how data augmentation is typically applied: via a random sequence of transformations. In this section we model this augmentation procedure as a Markov process.

approximation indeed provides a better approximation. For LeNet (Appendix E), the results are quite similar, though we additionally observe that the first-order approximation is very close to the model trained without augmentation, suggesting that the data-dependent regularization of the second-order term may be the dominating effect in models with learned feature maps.

4 Data Augmentation as a Kernel

As illustrated in Section 3, the effect of complex augmentations, such as non-local transformations and sequences of composed transformations, is not captured as well by the derived first- and second-order approximations. While recent work has attempted to better incorporate these complex transformations algorithmically [28, 7, 21, 19], our intent here is instead explanatory. In particular, to understand the effect of these transformations, we propose and investigate a novel model for data augmentation as a Markov process, inspired by the manner in which data augmentation is typically applied—via the composition of multiple different types of transformations. Surprisingly, we show this augmentation model combined with a k -nearest neighbor (k -NN) classifier is asymptotically equivalent to a kernel classifier, where the kernel is a function only of the augmentation process. In other words, kernels appear naturally in relation to data augmentation, even when we don’t start with a kernel classifier. Beyond serving as theoretical understanding of the effect of augmentation, we discuss the practicality of our model and how our results motivate alternate ways to optimize the composed augmentation process (Section 4.3).

4.1 Markov Chain Augmentation Process

In data augmentation, the aim is to perform class-preserving transformations to the original training data to improve generalization. As a concrete example, a classifier that correctly predicts an image of the number ‘3’ should be able to predict this number whether or not the image is slightly rotated, translated, or blurred. It is therefore common to pick some number of augmentations (e.g., for images: flip, rotation, zoom, blur, additive noise, etc.), and to create synthetic examples by taking an original data point and applying a *sequence* of composed augmentations. Figure 2 illustrates an example augmentation sequence on an image datapoint.

To model this process, we consider the following procedure: given a data point, we repeatedly pick augmentations from a set of augmentations at random, and apply them one after the other. To avoid deviating too far from the training set, with some probability we discard the point and start over from a random point in the original dataset. This augmentation process can be formalized via a Markov chain as follows.

Definition 1 (Markov chain augmentation model). Consider the problem of learning a classifier mapping a finite domain \mathcal{X} to a set of labels $\mathcal{Y} = \{-1, 1\}$.² Given a dataset of D examples $z_i = (x_i, y_i) \in \mathcal{X} \times \mathcal{Y}$, the goal is to augment the dataset using some *augmentation matrices* $A_1, A_2, \dots, A_m, A_i \in \mathbb{R}^{\Omega \times \Omega}$, which are stochastic transition matrices over the state space of possible labeled examples $\Omega = \mathcal{X} \times \mathcal{Y}$. We model this by constructing a discrete time Markov chain on Ω that has the following transitions:

- With probability proportional to β_i , an *augmentation transition* occurs, using the augmentation matrix A_i .

²Although in theory we typically think of continuous domains such as \mathbb{R}^d , in practice the space can be divided into a finite number of local regions; working with floating point numbers automatically has this effect.

- With probability proportional to γ_j , a *retraction* to the training set occurs, and the state is reset to z_j .

Finally, without loss of generality, we let all rates be normalized with $\sum_j \gamma_j = 1$, so that γ_j represents a distribution over the original training data. To formalize this, we make the following *surjectivity assumption*: We assume every state $z \in \Omega$ can be produced from a starting example through some sequence of augmentations. This assumption, which will allow the chain to be ergodic, is not restrictive in the sense that while all states must be reachable, the probability of reaching distant states will tend towards zero in practice. For example, any sort of jitter (additive noise) transformation satisfies this condition.

The transition matrix for the Markov chain is given in Proposition 1. From Definition 1, by conditioning on which transition is chosen, it is evident that the entire process is equivalent to a Markov chain whose transition matrix is the weighted average of the base transitions. Our surjectivity assumption (combined with the fact that the chain can retract to any training example at any timestep) implies that the chain is both irreducible and aperiodic, hence ergodic.

Proposition 1. *The augmentation process is a Markov chain with transition matrix*

$$R = \left(1 + \sum_{i=1}^m \beta_i\right)^{-1} \left[\sum_{i=1}^m \beta_i A_i + \sum_{j=1}^D \gamma_j \left(1e_{z_j}^\top\right) \right].$$

Using this transition matrix, we derive the following unique stationary distribution of the Markov chain, which reflects the asymptotic distribution of the augmented dataset.

Lemma 1 (Stationary distribution). *The stationary distribution is given by*

$$\pi = \rho^\top (I(\beta + 1) - A)^{-1}, \quad (4)$$

where

$$A = \sum_{i=1}^m \beta_i A_i, \quad \beta = \sum_{i=1}^m \beta_i, \quad \rho = \sum_{j=1}^D \gamma_j e_{z_j}.$$

We prove Lemma 1 in Appendix B. Note that it agrees intuitively with the augmentation process in the following way: When $\beta_i \approx 0$ (i.e. low rate of augmentation), Lemma 1 implies that the stationary distribution π is very close to ρ , the original data distribution. As β_i increases, the stationary distribution is increasingly distorted by the augmentations.

4.2 Classification Yields a Kernel

Using our proposed model of augmentation, we now show that classifying an unseen example using augmented data results in a kernel classifier. In doing so, we can observe the effect that augmentation has on the learned feature representation of the original data. We discuss some additional uses and extensions of the result itself in Section 4.3.

Theorem 1. *Consider running the Markov chain augmentation process in Definition 1 where the base augmentations preserve labels, and classifying an unseen example $y \in \Omega$ using k -nearest neighbors. Then there are coefficients $\psi(z_i)$ and a kernel K depending only on the augmentations, such that in the limit as the number of augmented examples goes to infinity, this classification procedure is equivalent to a kernel classifier*

$$\hat{y} = \text{sign} \sum_{i=1}^D y_i \psi(z_i) K(x_i, x). \quad (5)$$

We outline the proof below; for details see Appendix B.

Classification process. Suppose that we receive a new example $x \in \mathcal{X}$ with unknown label y . Consider running the augmentation process for time T and determining the label for x via k -nearest neighbors.³ Then in the limit as $T \rightarrow \infty$, the surjectivity assumption from Section 4.1 implies that every example will be generated, and we predict

$$\hat{y} = \arg \max_{y \in \mathcal{Y}} \pi((x, y)). \quad (6)$$

In other words, as the number of augmented training examples increases, k -NN approaches a Bayes classifier: it will select the class for x that is most probable in π .

We now show that under additional mild assumptions on the base augmentations A_i , applying this classification process after the Markov chain augmentation process is equivalent to a kernel classifier. In particular, *suppose that the Markov chains corresponding to the A_i are all time-reversible and there is a positive distribution π_0 that is stationary for all A_i .* This condition is not restrictive in practice, as we discuss in Section 4.3. Under these assumptions, the stationary distribution can be expressed in terms of a kernel matrix.

Lemma 2. *The stationary distribution (4) can be written as $\pi = \psi^\top K$, where the vector $\psi \in \mathbb{R}^\Omega$ is supported only on the dataset z_1, \dots, z_D , and K is a kernel matrix (i.e. K symmetric positive definite and non-negative) depending only on the augmentations A_i, β_i .*

By Lemma 2, since ψ is supported only on the training set z_1, \dots, z_D , the stationary probabilities can be expressed as $\pi(z) = \sum_{u \in \Omega} \psi(u)K(u, z) = \sum_{i=1}^D \psi(z_i)K(z_i, z)$.

Expanding the classification rule (6) using this explicit representation yields

$$\begin{aligned} \hat{y} &= \arg \max_{y \in \{-1, 1\}} \sum_{i=1}^D \psi(z_i)K((x_i, y_i), (x, y)) \\ &= \text{sign} \sum_{y \in \{-1, 1\}} y \sum_{i=1}^D \psi(z_i)K((x_i, y_i), (x, y)). \end{aligned}$$

Finally, suppose, as is common practice, that our augmentations A_i do not change the label y .⁴ In this case, we overload the notation K so that $K(x_1, x_2) := K((x_1, 1), (x_2, 1)) = K((x_1, -1), (x_2, -1))$, and the classification simplifies to equation (5),

the classification rule for a kernel-trick linear classifier using kernel K . Thus, *k -NN with data augmentation is asymptotically equivalent to a kernel classifier*.

Rate of Convergence. The rate at which the augmentation plus k -NN classifier approaches the kernel classifier can be decomposed into two parts: the rate at which the augmentation Markov chain mixes, and the rate at which the k -NN classifier approaches the true function. The latter follows from standard generalization error bounds for the k -NN classifier. For example, if the kernel regression function $L(x) = \sum_{i=1}^D \psi(z_i)K(x_i, x)$ is smooth enough (e.g. Lipschitz) on the underlying space $\mathcal{X} = \mathbb{R}^d$, then the expected difference between the two classifiers of the probability of misclassifying new examples scales as $n^{-1/(2+d)}$, where n is the number of samples (i.e. augmentation steps) [10]. Furthermore, the stationary distribution (4) can be further analyzed to yield the finite-sample distributions of the Markov chain, which is related to the power series expansion $\rho^\top(I(\beta+1) - A)^{-1} = \rho^\top(\beta+1)^{-1}(I + A/(\beta+1) + \dots)$ of Equation (4). This in turn determines the mixing rate of the Markov chain, which converges to its stationary distribution exponentially fast with rate $\beta/(\beta+1)$. More formal statements and proofs of these bounds are in Appendix B.1.

4.3 Discussion

Here we describe our modeling assumptions in more detail, as well as additional uses of our main result in Theorem 1. First, we note that the assumptions needed for Lemmas 1 and 2 are much broader than the

³This works for any label-preserving non-parametric model.

⁴This is not at odds with the surjectivity assumption on the Markov chain, since for effective augmentations the probability of transitioning to a label-changing state is vanishingly small.

assumptions in Section 3, and hold for most transformations used in practice. For example, the condition behind Lemma 2 is satisfied by “reversible” augmentations, or any augmentation that has equal probability of sending a point $x \in \Omega$ to y as y to x : these augmentations have symmetric transition matrices, which are time-reversible and have a uniform stationary distribution. This class includes all deterministic lossless transformations, such as jittering, flips, and rotations for images. Furthermore, lossy transformations can be combined with their inverse transformation (such as `ZoomOut` for `ZoomIn`), possibly adding a probability of not transitioning, to form a symmetric augmentation.⁵

Beyond serving as motivation for analyzing data augmentation in conjunction with kernel classifiers, Theorem 1 also points to alternate ways to understand and optimize the augmentation pipeline. Lemma 2 provides a closed-form representation for the induced kernel in terms of the base augmentation matrices and rates, and we point out two potential ways this alternate classifier can be useful on top of the original augmentation process.

In Appendix C.1 we show that if the augmentations are changed, for example by tuning the rates or adding/removing a base augmentation, the kernel matrix can potentially be directly updated from the original kernel (opposed to re-sampling an augmented dataset and re-training the classifier).

Second, many parameters of the original process appear in the kernel directly. For example, in Appendix C.2 we show that in the simple case of a single additive Gaussian noise augmentation, the equivalent kernel is very close to a Gaussian kernel whose bandwidth is a function of the variance of the jitter. Additionally, in general the augmentation rates β_i all show up in the resulting kernel in a differentiable manner. Therefore instead of treating them as hyperparameters, there is potential to optimize the underlying parameters in the base augmentations, as well as the augmentation rates, through their role in a more tractable objective.

5 Practical Connections: Accelerating Training with Data Augmentation

We now demonstrate two applications of our proposed framework, both serving as practical ways to accelerate deep neural network training with data augmentation: First, we explore reducing training computation via feature averaging at intermediate layers, and second, we propose a kernel similarity metric that can be used to quickly predict the utility of potential augmentations. We consider the setting where the classifier is a neural network, which can be seen as a kernel classifier with learned feature map. If all but the last layer of the network are fixed (e.g., during fine tuning), our theory holds exactly. When the approximation is applied at earlier layers, our theory does not hold due to the non-convexity of the objective. However, we demonstrate that it still can still be used in practice, and as additional motivation for this transition, we provide experiments in Appendix E.2 that show the per-layer effects in a deep network, where we observe that data augmentation indeed increases feature invariance to the utilized augmentation at each layer.

5.1 Intermediate-Layer Feature Averaging

The approximation developed in Section 3 involves averaging the features of augmented input points. If we perform this averaging at an intermediate layer of a deep neural network, all subsequent layers need only operate over the averaged signal, which suggests a way to increase the computational efficiency during training. Let the first k layers define a feature map ϕ , and let the remaining layers define a non-linear function $f(\phi(x))$. The loss on each data point is then of the form $\mathbf{E}_{z_i \sim T(x_i)} [l(f(\phi(z_i)); y_i)]$. Using the second-order Taylor expansion around $\psi(x_i) = \mathbf{E}_{z_i \sim T(x_i)} [\phi(z_i)]$, we obtain the approximate objective

$$\frac{1}{N} \sum_{i=1}^N l(f(\psi(x_i)); y_i) + \frac{1}{2} \mathbf{E}_{z_i \sim T(x_i)} [\phi(z_i) - \psi(x_i)(\phi(z_i) - \psi(x_i))^\top] \nabla_{\psi(x_i)}^2 l(f(\psi(x_i)); y_i),$$

⁵For example, if a lossy transform sends $a, b, c \rightarrow c$, with transition matrix $\begin{pmatrix} 0 & 0 & 1 \\ 0 & 0 & 1 \\ 0 & 0 & 1 \end{pmatrix}$, it can be symmetrized to $\begin{pmatrix} 2/3 & 0 & 1/3 \\ 0 & 2/3 & 1/3 \\ 1/3 & 1/3 & 1/3 \end{pmatrix}$.

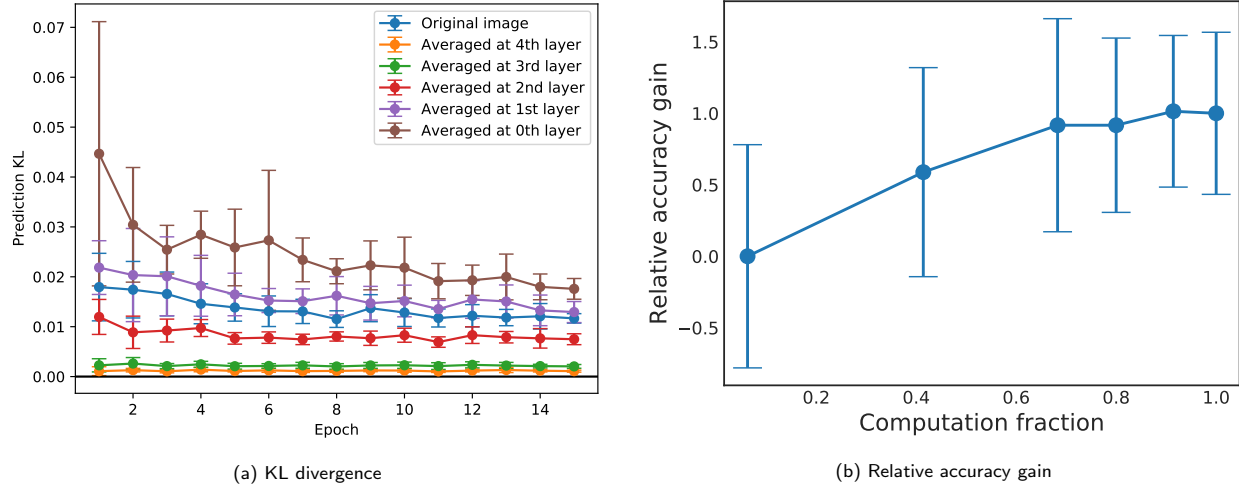


Figure 3: Difference in generalization between approximate and true objectives for LeNet. Approximation at earlier layers saves computation but reduces the fidelity of the approximation.

If $f(\phi(x)) = w^\top \phi(x)$, we recover the result in Section 3.

Connection to tangent propagation. Operationally, to approximate data augmentation, we carry out the forward pass on all transformed versions of the data points up to layer k (i.e., computing $\phi(z_i)$), then average the features and continue with the remaining layers using this average feature. If we do the averaging before the very first layer and use the analytic form of the gradient with respect to the transformations, which are called *tangent vectors*, then we recover *tangent propagation*. The connection between data augmentation and tangent propagation in this special case was observed by Zhao et al. [32].

Accuracy vs. computation trade-off. We explore the effect of training with approximation objectives, this time at various layers of a LeNet network using rotation as the augmentation. In Figure 3a, we plot the Kullback–Leibler divergence between the distribution over classes predicted by the true model and the approximate models (averaged at different layers of the network). Averaging at the last layer yields very similar prediction to the true model, as reflected by the high prediction agreement and low KL divergence. However, as we perform feature averaging at earlier layers, the approximation gets worse. This presents a trade-off between approximation accuracy and computation. To get a rough measure of trade-off, we record the fraction of computation time spent at each layer in the forward pass, and use this to measure the expected reduction in computation when approximating at layer k . In Figure 3b, we plot the relative accuracy gain of the classifier when trained on approximate objectives against the fraction of computation time, where 0 corresponds to accuracy (averaged over 10 trials) of training on original data and 1 corresponds to accuracy of training on true augmented objective $g(w)$. These results indicate, e.g., that approximating the objective can reduce computation by 30%, while maintaining 92% of the accuracy gain.

5.2 A Fast Kernel Metric for Augmentation Selection

Beyond reducing the training computation itself, we explore the potential to accelerate training by reducing the burden of augmentation tuning. For new tasks and datasets, manually selecting, tuning, and composing augmentations is one of the most time-consuming processes in optimizing a deep learning pipeline, yet is critical to achieving state-of-the-art performance. We propose a kernel alignment metric, motivated by our theoretical framework, for quickly estimating if a transformation is likely to improve generalization performance *without performing end-to-end training*.

Kernel alignment metric. Given a transformation T , and an original feature map $\phi(x)$ (e.g. learned from training once on non-augmented data), the new approximate features for each data point x are $\psi(x) = \mathbf{E}_{z \sim T(x)} [\phi(z)]$. Defining the feature kernel $\tilde{K}(x, x') = \psi(x)^\top \psi(x')$ and the label kernel $K_Y(y, y') = \mathbf{1}\{y = y'\}$,

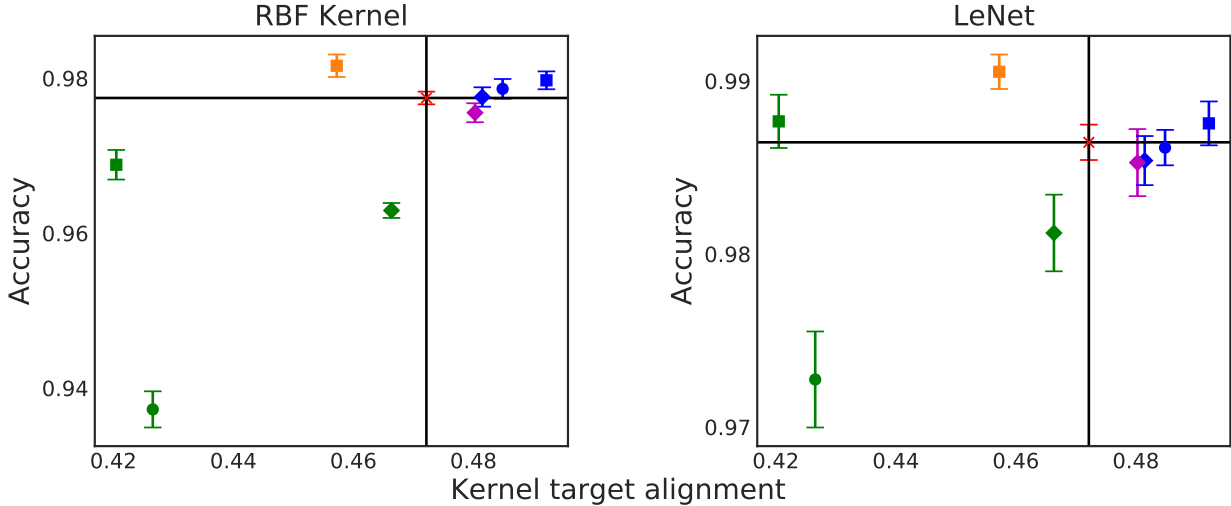
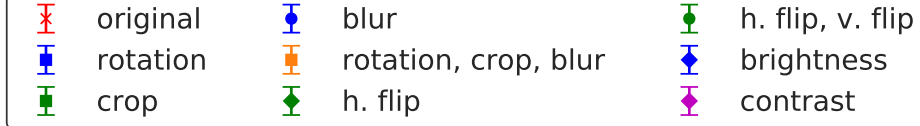


Figure 4: Accuracy vs kernel target alignment metric for RBF kernel and LeNet. This alignment metric can be used to select transformations (e.g., rotation, blur) that improve performance and avoid bad transformations (e.g., flips).

we can compute the *kernel target alignment* [2] between the feature kernel \bar{K} and the target kernel K_Y without training:

$$\hat{A}(X, \bar{K}, K_Y) = \frac{\langle \bar{K}, K_Y \rangle}{\sqrt{\langle \bar{K}, \bar{K} \rangle \langle K_Y, K_Y \rangle}},$$

where $\langle K_a, K_b \rangle = \sum_{i,j}^N K_a(x_i, x_j) K_b(x_i, x_j)$. This alignment statistic can be estimated quickly and accurately from subsamples of the data [2]. The kernel target alignment measures the extent to which points in the same class have similar features. If this alignment is larger than that between the original feature kernel $K(x, x') = \phi(x)^\top \phi(x)$ and the target kernel, we postulate that the transformation T is likely to improve generalization. We validate this method on MNIST with numerous transformations (rotation, crop, blur, flip, brightness, and contrast); full details are provided in Appendix E.3. In Figure 4, we plot the accuracy of the kernel classifier and LeNet against the kernel target alignment. There is a general correlation between kernel alignment and accuracy, as the points are clustered in the upper right (higher alignment, higher accuracy) and lower left (lower alignment, lower accuracy) quadrants. Outliers to the general correlation involve non-local or sequence transformations that are not well-approximated by the first-order term (Section 3).

6 Conclusion

We have taken steps to establish a firm footing for modern data augmentation techniques. We show that simple local transformations for data augmentation can be approximated by first-order feature averaging and second-order variance regularization components, having the rough effects of increasing coverage of invariant forms and reducing model complexity. For more complex transformations, we analyze a novel Markov process model and show that the k -nearest neighbors classifier applied to augmented data is asymptotically equivalent to a kernel classifier, illustrating the effect that augmentation has on the learned features of the original data. We use our insights to suggest ways to accelerate training for kernel and deep learning pipelines.

Finally, we note promising directions of future work. The analysis in Section 4 may provide a process by which

to derive analytic correspondence between kernels and corresponding transformations, which would further reduce the burden of augmentation. Hyperparameters of the transformations may also enter the feature map in a differentiable manner, allowing automatic optimization of these hyperparameters directly. Generally, a tension exists between incorporating domain knowledge more naturally via data augmentation, or in a better-studied manner through kernel approaches. We hope our work will enable easier translation between these two extremes, leading to more principled and theoretically grounded application of data augmentation.

Acknowledgments

We thank Fred Sala and Madalina Fiterau for helpful discussion, and Avner May for providing detailed feedback on earlier versions.

This material is based on research sponsored by Defense Advanced Research Projects Agency (DARPA) under agreement number FA8750-17-2-0095. We gratefully acknowledge the support of the DARPA SIMPLEX program under No. N66001-15-C-4043, DARPA FA8750-12-2-0335 and FA8750-13-2-0039, DOE 108845, National Institute of Health (NIH) U54EB020405, the National Science Foundation (NSF) under award No. CCF-1563078, the Office of Naval Research (ONR) under awards No. N00014-17-1-2266, the Moore Foundation, the Okawa Research Grant, American Family Insurance, Accenture, Toshiba, and Intel. This research was supported in part by affiliate members and other supporters of the Stanford DAWN project: Intel, Microsoft, Teradata, and VMware. The U.S. Government is authorized to reproduce and distribute reprints for Governmental purposes notwithstanding any copyright notation thereon. The views and conclusions contained herein are those of the authors and should not be interpreted as necessarily representing the official policies or endorsements, either expressed or implied, of DARPA or the U.S. Government. Any opinions, findings, and conclusions or recommendations expressed in this material are those of the authors and do not necessarily reflect the views of DARPA, AFRL, NSF, NIH, ONR, or the U.S. government.

References

- [1] Cireşan, Dan Claudiu, Meier, Ueli, Gambardella, Luca Maria, and Schmidhuber, Jürgen. Deep, big, simple neural nets for handwritten digit recognition. *Neural Computation*, 22(12):3207–3220, 2010.
- [2] Cristianini, Nello, Shawe-Taylor, John, Elisseeff, Andre, and Kandola, Jaz S. On kernel-target alignment. In *Neural Information Processing Systems*, 2002.
- [3] Decoste, Dennis and Schölkopf, Bernhard. Training invariant support vector machines. *Machine Learning*, 46(1):161–190, 2002.
- [4] Demyanov, Sergey, Bailey, James, Kotagiri, Ramamohanarao, and Leckie, Christopher. Invariant backpropagation: how to train a transformation-invariant neural network. *arXiv:1502.04434*, 2015.
- [5] Dosovitskiy, Alexey, Springenberg, Jost Tobias, Riedmiller, Martin, and Brox, Thomas. Discriminative unsupervised feature learning with convolutional neural networks. In *Neural Information Processing Systems*, 2014.
- [6] Dosovitskiy, Alexey, Fischer, Philipp, Springenberg, Jost Tobias, Riedmiller, Martin, and Brox, Thomas. Discriminative unsupervised feature learning with exemplar convolutional neural networks. *IEEE Transactions on Pattern Analysis and Machine Intelligence*, 38(9):1734–1747, 2016.
- [7] Fawzi, Alhussein, Samulowitz, Horst, Turaga, Deepak, and Frossard, Pascal. Adaptive data augmentation for image classification. In *International Conference on Image Processing*, 2016.
- [8] Goodfellow, Ian, Bengio, Yoshua, and Courville, Aaron. *Deep Learning*. MIT Press, 2016. <http://www.deeplearningbook.org>.
- [9] Graham, Benjamin. Fractional max-pooling. *arXiv:1412.6071*, 2014.

[10] Györfi, László, Kohler, Michael, Krzyzak, Adam, and Walk, Harro. *A distribution-free theory of nonparametric regression*. Springer Science & Business Media, 2006.

[11] Haasdonk, Bernard and Burkhardt, Hans. Invariant kernel functions for pattern analysis and machine learning. *Machine Learning*, 68(1):35–61, 2007.

[12] He, Kaiming, Zhang, Xiangyu, Ren, Shaoqing, and Sun, Jian. Identity mappings in deep residual networks. In *European Conference on Computer Vision*, 2016.

[13] LeCun, Yann, Bottou, Léon, Bengio, Yoshua, and Haffner, Patrick. Gradient-based learning applied to document recognition. *Proceedings of the IEEE*, 86(11):2278–2324, 1998.

[14] Leen, Todd. From data distributions to regularization in invariant learning. In *Neural Information Processing Systems*, 1995.

[15] Lu, Xinghua, Zheng, Bin, Velivelli, Atulya, and Zhai, ChengXiang. Enhancing text categorization with semantic-enriched representation and training data augmentation. *Journal of the American Medical Informatics Association*, 13(5):526–535, 2006.

[16] Maurer, Andreas and Pontil, Massimiliano. Empirical Bernstein bounds and sample variance penalization. In *Conference on Computational Learning Theory*, 2009.

[17] Namkoong, Hongseok and Duchi, John. Stochastic gradient methods for distributionally robust optimization with f-divergences. In *Neural Information Processing Systems*, 2016.

[18] Namkoong, Hongseok and Duchi, John C. Variance-based regularization with convex objectives. In *Neural Information Processing Systems*, 2017.

[19] Pal, Dipan, Kannan, Ashwin, Arakalgud, Gautam, and Savvides, Marios. Max-margin invariant features from transformed unlabelled data. In *Neural Information Processing Systems*, 2017.

[20] Rahimi, Ali and Recht, Benjamin. Random features for large-scale kernel machines. In *Neural Information Processing Systems*, 2007.

[21] Ratner, Alexander J, Ehrenberg, Henry, Hussain, Zeshan, Dunnmon, Jared, and Ré, Christopher. Learning to compose domain-specific transformations for data augmentation. In *Neural Information Processing Systems*, 2017.

[22] Rifai, Salah, Dauphin, Yann N, Vincent, Pascal, Bengio, Yoshua, and Muller, Xavier. The manifold tangent classifier. In *Neural Information Processing Systems*, 2011.

[23] Sajjadi, Mehdi, Javanmardi, Mehran, and Tasdizen, Tolga. Regularization with stochastic transformations and perturbations for deep semi-supervised learning. In *Neural Information Processing Systems*, 2016.

[24] Schölkopf, Bernhard, Burges, Chris, and Vapnik, Vladimir. Incorporating invariances in support vector learning machines. In *International Conference on Artificial Neural Networks*, 1996.

[25] Sietsma, Jocelyn and Dow, Robert JF. Creating artificial neural networks that generalize. *Neural Networks*, 4(1):67–79, 1991.

[26] Simard, Patrice, Victorri, Bernard, LeCun, Yann, and Denker, John. Tangent prop-a formalism for specifying selected invariances in an adaptive network. In *Neural Information Processing Systems*, 1992.

[27] Simard, Patrice, LeCun, Yann, Denker, John, and Victorri, Bernard. Transformation invariance in pattern recognition: tangent distance and tangent propagation. *Neural Networks: Tricks of the Trade*, pp. 549–550, 1998.

[28] Teo, Choon H, Globerson, Amir, Roweis, Sam T, and Smola, Alex J. Convex learning with invariances. In *Neural Information Processing Systems*, 2008.

- [29] Tibshirani, Ryan and Wasserman, Larry. Nonparametric regression and classification, 2018. URL <http://www.stat.cmu.edu/~larry/=sml/NonparametricPrediction.pdf>.
- [30] Uhlich, S., Porcu, M., Giron, F., Enenkl, M., Kemp, T., Takahashi, N., and Mitsufuji, Y. Improving music source separation based on deep neural networks through data augmentation and network blending. In *International Conference on Acoustics, Speech and Signal Processing*, 2017.
- [31] Zhang, Chiyuan, Bengio, Samy, Hardt, Moritz, Recht, Benjamin, and Vinyals, Oriol. Understanding deep learning requires rethinking generalization. In *International Conference on Learning Representations*, 2017.
- [32] Zhao, Jian, Li, Jianshu, Zhao, Fang, Yan, Shuicheng, and Feng, Jiashi. Marginalized CNN: Learning deep invariant representations. In *British Machine Vision Conference*, 2017.

A Additional Propositions for Section 3

A function f is α -strongly convex if for all x and x' , $f(x') \geq f(x) + \nabla f(x)^\top (x' - x) + (\alpha/2) \|x' - x\|^2$; the function f is β -strongly smooth if for all x and x' , $f(x') \leq f(x) + \nabla f(x)^\top (x' - x) + (\beta/2) \|x' - x\|^2$.

If we assume that the loss is strongly convex and strongly smooth, then the difference in objective functions $g(w)$ and $\hat{g}(w)$ can be bounded in terms of the squared-norm of w , and then the minimizer of the approximate objective $\hat{g}(w)$ is close to the minimizer of the true objective $g(w)$.

Proposition 2. *Assume that the loss function $l(x; y)$ is α -strongly convex and β -strongly smooth with respect to x , and that*

$$\begin{aligned} aI \preceq \frac{1}{N} \sum_{i=1}^N \mathbf{Cov}_{z_i \sim T(x_i)} (\phi(z_i)) \preceq bI, \quad \text{and} \\ \frac{1}{N} \sum_{i=1}^N \psi(x_i) \psi(x_i)^\top \succeq cI. \end{aligned}$$

Letting $w^* = \arg \min g(w)$ and $\hat{w} = \arg \min \hat{g}(w)$, then

$$\begin{aligned} \frac{\alpha a}{2} \|w\|^2 \leq g(w) - \hat{g}(w) \leq \frac{\beta b}{2} \|w\|^2, \quad \text{and} \\ \|w^* - \hat{w}\|^2 \leq \frac{\beta b}{\alpha c} \|\hat{w}\|^2. \end{aligned}$$

If $\alpha c \gg \beta b$ (that is, the covariance of $\phi(z_i)$ is small relative to the square of its expected value), then $\frac{\beta b}{\alpha c} \ll 1$, and so

$$\|w^* - \hat{w}\|^2 \ll \|\hat{w}\|^2.$$

This means that minimizing the first-order approximate objective \hat{g} will provide a fairly accurate parameter estimate for the objective g on the augmented dataset.

Proof of Proposition 2. By Taylor's theorem, for any random variable X over \mathbb{R} , there exists some remainder function $\zeta : \mathbb{R} \rightarrow \mathbb{R}$ such that

$$\begin{aligned} \mathbf{E} [l(X; y)] &= \mathbf{E} \left[l(\mathbf{E}[X]; y) + (X - \mathbf{E}[X])l'(\mathbf{E}[X]; y) + \frac{1}{2}(X - \mathbf{E}[X])^2 l''(\zeta(X); y) \right] \\ &= l(\mathbf{E}[X]; y) + \frac{1}{2} \mathbf{E} [(X - \mathbf{E}[X])^2 l''(\zeta(X); y)]. \end{aligned}$$

The condition of $l(x; y)$ being α -strongly convex and β -strongly smooth means that $\alpha \leq l''(x) \leq \beta$ for any x . Thus

$$\frac{\alpha}{2} \mathbf{Var}(X) \leq \mathbf{E} [l(X)] - l(\mathbf{E}[X]) \leq \frac{\beta}{2} \mathbf{Var}(X).$$

It follows that (letting our random variable X be $w^\top \phi(z_i)$),

$$\frac{\alpha}{2} \cdot \frac{1}{N} \sum_{i=1}^N \mathbf{Var}_{z_i \sim T(x_i)} (w^\top \phi(z_i)) \leq g(w) - \hat{g}(w) \leq \frac{\beta}{2} \cdot \frac{1}{N} \sum_{i=1}^N \mathbf{Var}_{z_i \sim T(x_i)} (w^\top \phi(z_i)).$$

Because of the assumption that $aI \preceq \frac{1}{N} \sum_{i=1}^N \mathbf{Cov}_{z_i \sim T(x_i)} (\phi(z_i)) \preceq bI$,

$$\frac{\alpha a}{2} \|w\|^2 \leq g(w) - \hat{g}(w) \leq \frac{\beta b}{2} \|w\|^2.$$

We can bound the second derivative of $\hat{g}(w)$:

$$\begin{aligned}\nabla^2 \hat{g}(w) &= \frac{1}{N} \sum_{i=1}^N \psi(x_i) \psi(x_i)^\top l''(w^\top \psi(x_i); y_i) \\ &\succeq \frac{\alpha}{N} \sum_{i=1}^N \psi(x_i) \psi(x_i)^\top \\ &\succeq \alpha c,\end{aligned}$$

where we have used the assumption that $\frac{1}{N} \sum_{i=1}^N \psi(x_i) \psi(x_i)^\top \succeq cI$. Thus \hat{g} is (αc) -strongly convex.

We bound $\hat{g}(w^*) - \hat{g}(\hat{w})$:

$$\begin{aligned}\hat{g}(w^*) - \hat{g}(\hat{w}) &= \hat{g}(w^*) - g(w^*) + g(w^*) - g(\hat{w}) + g(\hat{w}) - \hat{g}(\hat{w}) \\ &\leq 0 + 0 + \frac{\beta b}{2} \|\hat{w}\|^2,\end{aligned}$$

where we have used the fact that $\hat{g}(w) \leq g(w)$ for all w and that w^* minimizes $g(w)$. But \hat{g} is (αc) -strongly convex, so $\hat{g}(w^*) - \hat{g}(\hat{w}) \geq \alpha c/2 \|w^* - \hat{w}\|^2$. Combining these inequalities yields

$$\|w^* - \hat{w}\|^2 \leq \frac{\beta b}{\alpha c} \|\hat{w}\|^2.$$

□

B Omitted Proofs from Section 4

Proof of Lemma 1. Recall that the stationary distribution satisfies $\pi R = \pi$.

Under the given notation, we can express R as

$$R = \frac{A + \mathbf{1}\rho^\top}{\beta + 1}.$$

Assume for now that $I(\beta + 1) - A$ is invertible. Notice that

$$\begin{aligned}\rho^\top (I(\beta + 1) - A)^{-1} \frac{A}{\beta + 1} &= \rho^\top (I(\beta + 1) - A)^{-1} \left(\frac{A - I(\beta + 1)}{\beta + 1} + I \right) \\ &= -\frac{\rho^\top}{\beta + 1} + \rho^\top (I(\beta + 1) - A)^{-1}\end{aligned}$$

Also, note that $A\mathbf{1} = \sum_i \beta_i (A_i \mathbf{1}) = \beta \mathbf{1}$, so we know that $(I(\beta + 1) - A)\mathbf{1} = \mathbf{1}$. So the inverse satisfies $(I(\beta + 1) - A)^{-1}\mathbf{1} = \mathbf{1}$ as well. Thus,

$$\begin{aligned}\rho^\top (I(\beta + 1) - A)^{-1} R &= \rho^\top (I(\beta + 1) - A)^{-1} \frac{A}{\beta + 1} + \rho^\top \frac{\mathbf{1}\rho^\top}{\beta + 1} \\ &= -\frac{\rho^\top}{\beta + 1} + \rho^\top (I(\beta + 1) - A)^{-1} + \frac{\rho^\top}{\beta + 1} \\ &= \rho^\top (I(\beta + 1) - A)^{-1}\end{aligned}$$

It follows that $\pi = \rho^\top (I(\beta + 1) - A)^{-1}$ is the stationary distribution of this chain.

Finally, we show that $I(\beta + 1) - A$ is invertible as follows. By the Gershgorin Circle Theorem, the eigenvalues of A lie in the union of the discs $B(A_{ii}, \sum_{j \neq i} |A_{ij}|) = B(A_{ii}, \beta - A_{ii})$. In particular, the eigenvalues have real part bounded by β . Thus $I(\beta + 1) - A$ has all eigenvalues with real part at least 1, hence is invertible. □

Proof of Lemma 2. Let $\Pi_0 = \text{diag}(\pi_0)$. The stationary distribution can be written as

$$\begin{aligned}\pi &= \rho^\top (I(\beta + 1) - A)^{-1} \\ &= \rho^\top (\Pi_0^{-1} \Pi_0 (\beta + 1) - \Pi_0^{-1} \Pi_0 A)^{-1} \\ &= \rho^\top \Pi_0 (\Pi_0 (\beta + 1) - \Pi_0 A)^{-1}\end{aligned}$$

(note that Π_0 is invertible from the assumption that π_0 is supported everywhere).

Letting $\psi = \Pi_0 \rho$ and $K = (\Pi_0 (\beta + 1) - \Pi_0 A)^{-1}$, we have $\pi = \psi^\top K$. Clearly, ψ is supported only on the dataset z_1, \dots, z_D since ρ is. It remains to show that K is a kernel.

The detailed balance condition of time-reversible Markov chains states that $\pi_0(u) A_i(u, v) = \pi_0(v) A_i(v, u)$ for all augmentations A_1, \dots, A_m and $u, v \in \Omega$. This condition implies $\Pi_0 A_i = (\Pi_0 A_i)^\top$, so that $\Pi_0 A_i$ is symmetric. This implies that $\Pi_0 A$ and in turn K are symmetric.

We showed in Lemma 1 that $I(\beta + 1) - A$ is positive definite. Using the characterization of A positive definite as $x^\top A x > 0 \forall x \neq 0$, this implies that $\Pi_0^{1/2} (I(\beta + 1) - A) \Pi_0^{1/2}$ is also positive definite. Conjugating by $\Pi_0^{1/2}$ implies that $\Pi_0 (I(\beta + 1) - A)$ and hence K is also positive definite.⁶

Finally, we need to show that $K = (I(\beta + 1) - A)^{-1}$ is a nonnegative matrix. Note that $\frac{1}{\beta} A$ is a stochastic matrix, hence the spectral radius of $\frac{A}{\beta+1}$ is bounded by $\frac{\beta}{\beta+1} < 1$. Therefore we can expand

$$\begin{aligned}K &= (I(\beta + 1) - A)^{-1} \\ &= \frac{1}{\beta + 1} \left(I - \frac{A}{\beta + 1} \right)^{-1} \\ &= \frac{1}{\beta + 1} \sum_{n=0}^{\infty} \left(\frac{A}{\beta + 1} \right)^n.\end{aligned}$$

This is a sum of nonnegative matrices, so K is nonnegative. \square

B.1 Convergence Rate

The following proposition from [10] and [29] provides generalization bounds for a k -NN classifier when $k \rightarrow \infty$ and $k/n \rightarrow 0$ at a suitable rate. Treating the equivalent kernel classifier as the true function, this bounds the risk between the k -NN and kernel classifiers as a function of the number of augmented samples n .

Proposition 3. *Let \hat{C} be the k -NN classifier. Let C_0 be the asymptotically equivalent kernel classifier from Theorem 1 and assume it is L -Lipschitz.*

Letting $r(C) = \Pr_{(x,y) \sim \pi}(y \neq C(x))$ be the risk of a classifier C , then

$$r(C) - r(C_0) \leq O(L^{d/(2+d)} n^{-1/(2+d)}).$$

Next we analyze the convergence of the Markov chain by computing its distribution at time n . Define

$$\pi_n = \frac{\rho^\top}{\beta + 1} \left(\frac{A^n}{(\beta + 1)^{n-1}} + \sum_{i=0}^{n-1} \left(\frac{A}{\beta + 1} \right)^i \right).$$

We claim that π_n is the distribution of the combined Markov augmentation process at time n .

Recall that ρ^\top is a distribution over the original training data. We naturally suppose that the initial example is drawn from this distribution, so that $\pi_0 = \rho^\top$. Note that this matches the expression for π_n at $n = 0$. All that remains to show that this is the distribution of the Markov chain at time n is to prove that $\pi_{n+1} = \pi_n R$.

⁶The positivity of K also follows from the Gershgorin circle theorem, similar to the use in proving Lemma 1.

From the relations $\rho^\top \mathbf{1} = 1$ and $A\mathbf{1} = \beta\mathbf{1}$, we have

$$\rho^\top A^i R = \rho^\top A^i \left(\frac{A + \mathbf{1}\rho^\top}{\beta + 1} \right) = \rho^\top \frac{A^{i+1} + \beta^i \rho^\top}{\beta + 1}$$

for all $i \geq 0$.

Therefore

$$\begin{aligned} \pi_n R &= \frac{\rho^\top}{\beta + 1} \left(\frac{A^n}{(\beta + 1)^{n-1}} + \sum_{i=0}^{n-1} \left(\frac{A}{\beta + 1} \right)^i \right) R \\ &= \frac{\rho^\top}{\beta + 1} \left(\frac{A^{n+1} + \beta^n I}{(\beta + 1)^n} + \sum_{i=0}^{n-1} \frac{A^{i+1} + \beta^i I}{(\beta + 1)^{i+1}} \right) \\ &= \frac{\rho^\top}{\beta + 1} \left(\frac{A^{n+1}}{(\beta + 1)^n} + \sum_{i=0}^{n-1} \frac{A^{i+1}}{(\beta + 1)^{i+1}} + \frac{\beta^n I}{(\beta + 1)^n} + \sum_{i=0}^{n-1} \frac{\beta^i I}{(\beta + 1)^{i+1}} \right) \\ &= \frac{\rho^\top}{\beta + 1} \left(\frac{A^{n+1}}{(\beta + 1)^n} + \sum_{i=1}^{n-1} \frac{A^i}{(\beta + 1)^i} + \frac{\beta^n I}{(\beta + 1)^n} + \frac{I}{\beta + 1} \frac{\left(1 - \left(\frac{\beta}{\beta+1}\right)^n\right)}{\left(1 - \frac{\beta}{\beta+1}\right)} \right) \\ &= \frac{\rho^\top}{\beta + 1} \left(\frac{A^{n+1}}{(\beta + 1)^n} + \sum_{i=1}^{n-1} \frac{A^i}{(\beta + 1)^i} + I \right) \\ &= \pi_{n+1}. \end{aligned}$$

The difference from the stationary distribution is

$$\begin{aligned} \pi_n - \pi &= \pi_n - \frac{\rho^\top}{\beta + 1} \sum_{i=0}^{\infty} \left(\frac{A}{\beta + 1} \right)^i \\ &= \frac{\rho^\top}{\beta + 1} \left(\frac{A^n}{(\beta + 1)^{n+1}} - \sum_{i=n}^{\infty} \left(\frac{A}{\beta + 1} \right)^i \right). \end{aligned}$$

The ℓ_2 norm of this can be straightforwardly bounded, noting that $\|A\|_{op} \leq \beta$.

$$\begin{aligned} \|\pi_n - \pi\|_2 &\leq \frac{1}{\beta + 1} \left(\frac{\beta^n}{(\beta + 1)^{(n+1)}} + \sum_{i=n}^{\infty} \left(\frac{\beta}{\beta + 1} \right)^i \right) \\ &\leq \frac{1}{\beta + 1} \left(\frac{\beta^n}{(\beta + 1)^{(n+1)}} + \frac{\beta^n}{(\beta + 1)^{n-1}} \right) \\ &= \left(\frac{\beta}{\beta + 1} \right)^n \left(1 + \frac{1}{(\beta + 1)^2} \right). \end{aligned}$$

A bound on the total variation distance instead incurs an extra constant (in the dimension). This shows that the augmentation chain mixes exponentially fast, i.e. takes $O((\beta + 1) \log(1/\varepsilon))$ samples to converge to a desired error from the stationary distribution.

C Kernel Transformations and Special Cases

C.1 Updated Kernel for Modified Augmentations

Our analysis of the kernel classifier in Lemma 2 yields a closed form in terms of the base augmentation matrices. This allows us to modify any kernel by changing the augmentations, producing a new kernel. For

example, imagine that we start with a kernel K , which has corresponding augmentation operator A such that

$$K = (I(\beta + 1) - A)^{-1}.$$

Suppose that we want to add an additional augmentation operator with stochastic transition matrix \hat{A} and rate $\hat{\beta}$. The resulting kernel is guaranteed to be a non-negative kernel by Lemma 2, and it can be computed from the known K by expanding

$$\begin{aligned} (I(\hat{\beta} + \beta + 1) - A - \hat{\beta}\hat{A}))^{-1} &= (K^{-1} + \hat{\beta}I - \hat{\beta}\hat{A})^{-1} \\ &= \left(\left[I + (I - \hat{A})\hat{\beta}K \right] K^{-1} \right)^{-1} \\ &= K \left(I + (I - \hat{A})\hat{\beta}K \right)^{-1} \\ &= K \sum_{n=0}^{\infty} \hat{\beta}^n ((\hat{A} - I)K)^n. \end{aligned}$$

C.2 Kernel Matrix for the Jitter Augmentation

In the context of Definition 1, consider performing a single augmentation A_i corresponding to adding Gaussian noise to an input vector. Although Definition 1 uses an approximated finite sample space, for this simple case we consider the original space $\mathcal{X} = \mathbb{R}^d$. The transition matrix A_1 is just the standard Gaussian kernel, $A_1(x, y) = (2\pi\sigma^2)^{-d/2} \exp(-\|x - y\|^2/(2\sigma^2))$. With rate β , the kernel matrix by Lemma 2 is

$$K = (I(1 + \beta) - \beta A)^{-1},$$

where we think of I as the identity operator on $\mathcal{X} \rightarrow \mathcal{X}$.

We define a d -dimensional Fourier Transform satisfying

$$\mathcal{F} \exp \left(-\frac{\|t\|^2}{2\sigma^2} \right) (\omega) = (\sigma^2)^{d/2} \exp \left(-\frac{\|\omega\|^2 \sigma^2}{2} \right).$$

Note that this Fourier Transform is its own inverse on Gaussian densities.

Therefore

$$\mathcal{F}K = \left[1 + \beta - \beta(2\pi)^{d/2} \exp \left(-\frac{\|\omega\|^2 \sigma^2}{2} \right) \right]^{-1}.$$

To compute the inverse transform of this, consider the function

$$\frac{1}{\alpha - \beta \exp \left(-\frac{\|t\|^2 \sigma^2}{2} \right)} = \frac{1}{\alpha} \left[\frac{1}{1 - \frac{\beta}{\alpha} \exp \left(-\frac{\|t\|^2 \sigma^2}{2} \right)} \right] = \frac{1}{\alpha} \left[1 + \sum_{i=1}^{\infty} \left(\frac{\beta}{\alpha} \right)^i \exp \left(\frac{-\|t\|^2 \sigma^2}{2} i \right) \right]$$

Applying the inverse Fourier Transform \mathcal{F}^{-1} , it becomes

$$\frac{1}{\alpha} \left[\delta(\omega) + \sum_{i=1}^{\infty} \left(\frac{\beta}{\alpha} \right)^i \frac{1}{(\sigma^2 i)^{d/2}} \exp \left(\frac{-\|t\|^2}{2\sigma^2 i} \right) \right].$$

Since the value of the kernel matrix only matters up to a constant, we can scale it by the first term. We also ignore the $\delta(\omega)$ term, which in the context of Theorem 1 only serves to emphasize that a test point in the training set should be classified as its known true label. Scaling by $\alpha(\alpha/\beta)\sigma^d$, we are left with

$$\begin{aligned} &\sum_{i=1}^{\infty} \left(\frac{\beta}{\alpha} \right)^{i-1} \frac{1}{i^{d/2}} \exp \left(\frac{-\|t\|^2}{2\sigma^2 i} \right) \\ &= \exp \left(\frac{-\|t\|^2}{2\sigma^2} \right) + \sum_{i=1}^{\infty} \left(\frac{\beta}{\alpha} \right)^i \frac{1}{(i+1)^{d/2}} \exp \left(\frac{-\|t\|^2}{2\sigma^2(i+1)} \right). \end{aligned}$$

Finally, after plugging in the corresponding values for α and β , notice that β is proportional to $(2\pi)^{-d/2}$, which causes the sum to be negligible.

D Variance Regularization Terms for Common Loss Functions

Here we derive the variance regularization term for common loss functions such as logistic regression and multinomial logistic regression.

For logistic regression,

$$\begin{aligned} l(x; y) &= \log(1 + \exp(-yx)) \\ &= -\frac{yx}{2} + \log\left(\exp\left(\frac{yx}{2}\right) + \exp\left(-\frac{yx}{2}\right)\right) \\ &= -\frac{yx}{2} + \log\left(2 \cosh\left(\frac{yx}{2}\right)\right) \\ &= -\frac{yx}{2} + \log 2 + \log \cosh\left(\frac{yx}{2}\right). \end{aligned}$$

And so

$$\begin{aligned} l'(x; y) &= -\frac{y}{2} + \frac{\sinh\left(\frac{yx}{2}\right)}{\cosh\left(\frac{yx}{2}\right)} \cdot \frac{y}{2} \\ &= -\frac{y}{2} + \frac{y}{2} \tanh\left(\frac{yx}{2}\right) \end{aligned}$$

and

$$\begin{aligned} l''(x; y) &= \frac{y^2}{4} \operatorname{sech}^2\left(\frac{yx}{2}\right) \\ &= \frac{1}{4} \operatorname{sech}^2\left(\frac{x}{2}\right), \end{aligned}$$

since $y \in \{-1, 1\}$ and so $y^2 = 1$. Therefore,

$$g(w) - \hat{g}(w) = w^\top \left(\frac{1}{4N} \sum_{i=1}^N \mathbf{E}_{z \sim T(x_i)} \left[(\phi(z) - \psi(x_i))(\phi(z) - \psi(x_i))^\top \sec^2\left(\frac{1}{2}\zeta_i(w^\top \phi(z))\right) \right] \right) w.$$

To second order, this is

$$\begin{aligned} g(w) - \hat{g}(w) &\approx w^\top \left(\frac{1}{4N} \sum_{i=1}^N \mathbf{E}_{z \sim T(x_i)} \left[(\phi(z) - \psi(x_i))(\phi(z) - \psi(x_i))^\top \sec^2\left(\frac{1}{2}(w^\top \psi(x_i))\right) \right] \right) w \\ &= w^\top \left(\frac{1}{4N} \sum_{i=1}^N \mathbf{Cov}_{z \sim T(x_i)} \left(\phi(z) \sec\left(\frac{1}{2}w^\top \psi(x_i)\right) \right) \right) w. \end{aligned}$$

For multinomial logistic regression, we use the cross entropy loss. With the softmax probability $p_i = \frac{\exp(x_i)}{\sum \exp(x_j)}$,

$$l(x; y) = -(x_y - \log \sum \exp(x_j)).$$

The first derivative is:

$$\nabla l(x; y) = \frac{\exp(x_i)}{\sum \exp(x_j)} - \mathbf{1}_{i=y} = p - \mathbf{1}_{i=y}.$$

The second derivative is:

$$\nabla^2 l(x; y) = \mathbf{diag}(p) - pp^T,$$

which does not depend on y .

E Additional Experiment Results

E.1 First- and Second-order Approximations for LeNet

For all experiments, we use the MNIST dataset and test three representative augmentations: rotations between -15 and 15 degrees, random crops of up to 64% of the image area, and Gaussian blur. We explore our approximation for kernel classifier models, using either an RBF kernel with random Fourier features [20] or a learned LeNet neural network [13] as our base feature map. We plot the mean and standard deviation over 10 runs. In Figure 5, we include the results using LeNet.

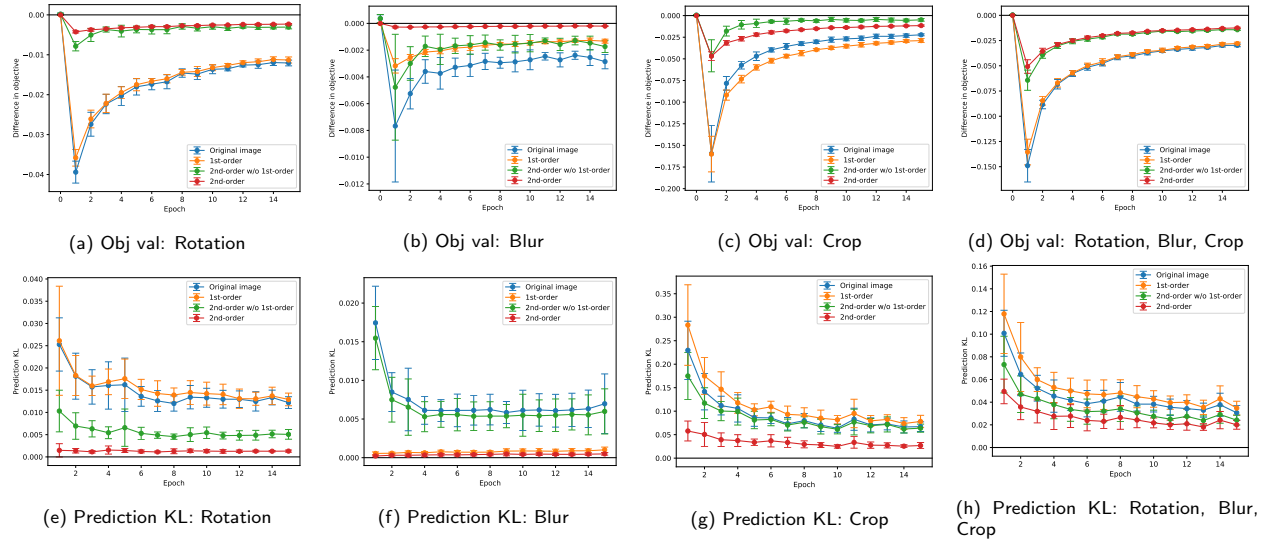


Figure 5: The difference in objective value (a-d) and prediction distribution (e-h) (as measured via the KL divergence) between approximate and true objectives during training, for LeNet. In all plots, the second-order approximation is much closer to the true objective than the first-order approximation, demonstrating that the variance regularization term (Section 3.3) plays a key role, particularly for LeNet as compared to RBF (Figure 1).

E.2 Layerwise Feature Invariance in a ResNet

For each layer l of a deep neural network, we examine the average difference in feature values when data points x are transformed according to a certain augmentation distribution T , using a model trained with data augmentation T' which has feature layers $\phi_l^{T'}$:

$$\Delta_{l,T,T'} = \sum_{i=1}^N \mathbf{E}_{z \sim T(x_i)} \left[\frac{1}{|\phi_l^{T'}(x_i)|} \|\phi_l^{T'}(x_i) - \phi_l^{T'}(z)\|^2 \right] \quad (7)$$

Specifically, in Figure 6, we examine the ratio of this measure of invariance for a model trained with data augmentation using T , and trained without any data augmentation, $\Delta_{l,T,T}/\Delta_{l,T,\emptyset}$, to see if and how training with a specific augmentation makes the layers of the network more invariant to it. We use a standard ResNet as in [12] with three blocks of nine residual units (separated by vertical dashed lines), an initial convolution layer, and a final global average pooling layer, implemented in TensorFlow⁷, trained on CIFAR-10 and averaged over ten trials. We see that training with an augmentation indeed makes the feature layers of the network more invariant to this augmentation, with the steepest change in the earlier layers (first residual block), and again in the final layer when features are pooled and averaged.

⁷<https://github.com/tensorflow/models/tree/master/official/resnet>

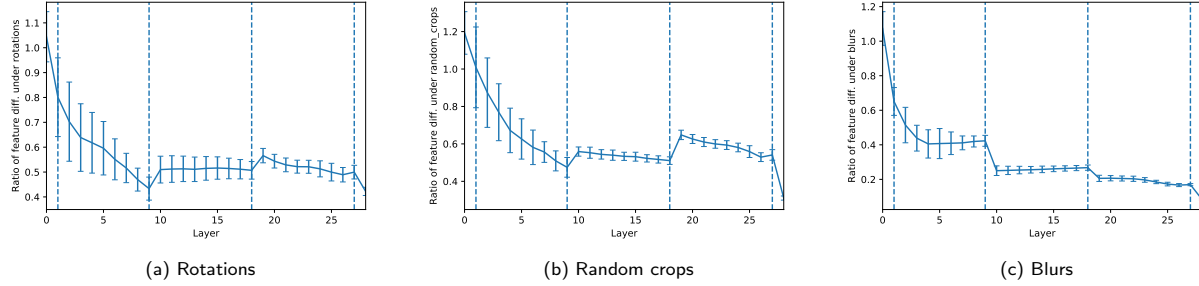


Figure 6: The ratio of average difference in features under an augmentation (7) when the network is trained with that augmentation, to when it is trained without any data augmentation, using a ResNet trained on CIFAR-10, averaged over ten trials. We see that in all but the first one or two layers, the network trained with the augmentation is indeed more invariant to it, with the steepest increase in invariance in the first block of layers and in the last global average pooling layer.

E.3 Kernel Target Alignment and Accuracy

We validate the correlation between accuracy and kernel target alignment on MNIST with rotation (between -15 and 15 degrees), random crop (up to 64% the area of the image), Gaussian blur, rotation & crop & blur, horizontal flip, horizontal & vertical flip, brightness adjustment (from 0.75 to 1.25 brightness factor), contrast adjustment (from 0.65 to 1.35 contrast factor). We report the result in Table 1. We see that kernel target alignment tends to correlate with higher accuracy (relative to no augmentation), making alignment a useful metric for measuring the utility of an augmentation prior to training.

Transform	Alignment	Kernel Acc.	LeNet Acc.
None	0.472	0.977	0.987
Rotation	0.492	0.980	0.988
Random crop	0.417	0.969	0.988
Blur	0.482	0.978	0.986
Rot., Crop, Blur	0.458	0.981	0.991
Horizontal flip	0.467	0.963	0.981
H. flip, V. flip	0.427	0.937	0.973
Brightness	0.480	0.978	0.985
Contrast	0.481	0.976	0.985

Table 1: Kernel target alignment and accuracy on MNIST. Larger kernel target alignment correlates with higher accuracy of the trained model.